Cell

The X-Linked Mental Retardation Gene *SMCX/JARID1C* Defines a Family of Histone H3 Lysine 4 Demethylases

Shigeki Iwase,[1,3] Fei Lan,[1,3] Peter Bayliss,[2,4] Luis de la Torre-Ubieta,[1,4] Maite Huarte,[1,4] Hank H. Qi,[2] Johnathan R. Whetstine,[1] Azad Bonni,[1] Thomas M. Roberts,[2] and Yang Shi[1,*]
[1] Department of Pathology, 77 Avenue Louis Pasteur
[2] Department of Cancer Biology, Dana-Farber Institute, 44 Binney Street
Harvard Medical School, Boston, MA 02115, USA
[3] These authors contributed equally to this work.
[4] These authors contributed equally to this work.
*Correspondence: yang_shi@hms.harvard.edu
DOI 10.1016/j.cell.2007.02.017

SUMMARY

Histone methylation regulates chromatin structure and transcription. The recently identified histone demethylase lysine-specific demethylase 1 (LSD1) is chemically restricted to demethylation of only mono- and di- but not trimethylated histone H3 lysine 4 (H3K4me3). We show that the X-linked mental retardation (XLMR) gene *SMCX* (*JARID1C*), which encodes a JmjC-domain protein, reversed H3K4me3 to di- and mono- but not unmethylated products. Other SMCX family members, including SMCY, RBP2, and PLU-1, also demethylated H3K4me3. SMCX bound H3K9me3 via its N-terminal PHD (plant homeodomain) finger, which may help coordinate H3K4 demethylation and H3K9 methylation in transcriptional repression. Significantly, several XLMR-patient point mutations reduced SMCX demethylase activity and binding to H3K9me3 peptides, respectively. Importantly, studies in zebrafish and primary mammalian neurons demonstrated a role for SMCX in neuronal survival and dendritic development and a link to the demethylase activity. Our findings thus identify a family of H3K4me3 demethylases and uncover a critical link between histone modifications and XLMR.

INTRODUCTION

Histone N-terminal tails are subject to a plethora of post-translational modifications, including phosphorylation, ubiquitination, acetylation, and methylation. Each modification can affect chromatin architecture, but the total sum of these modifications may be the ultimate determinant of the chromatin state, which governs gene transcription (Jenuwein and Allis, 2001; Strahl and Allis, 2000). Methylation occurs on both lysine (K) and arginine (R) residues. Five K residues on the tails of histones H3 and H4 (H3K4, -9, -27, -36, and H4K20) as well as K79 located within the core of histone H3 have been shown to be sites for methylation (Margueron et al., 2005; Zhang and Reinberg, 2001). Lysine methylation exists in three different states, including mono-, di-, or trimethylation, which may bring about additional regulatory complexity. Histone methylation has been linked to transcriptional activation and repression, as well as DNA-damage response (Sanders et al., 2004; Zhang and Reinberg, 2001). It has also been implicated in heterochromatin formation, X inactivation, genomic imprinting, and silencing of homeotic genes, demonstrating an important role for histone methylation in multiple biological processes (Martin and Zhang, 2005). Until recently, histone methylation was considered enzymatically irreversible. However, the recent discovery of a large number of histone demethylases indicates that demethylases play a central role in the regulation of histone methylation dynamics (Cloos et al., 2006; Fodor et al., 2006; Klose et al., 2006b; Metzger et al., 2005; Shi et al., 2004; Tsukada et al., 2006; Whetstine et al., 2006; Yamane et al., 2006).

Histone H3K4 trimethylation positively regulates transcription (Liang et al., 2004; Litt et al., 2001; Noma et al., 2001; Santos-Rosa et al., 2002; Schneider et al., 2004) in part by recruiting chromatin-remodeling complexes (Santos-Rosa et al., 2003; Wysocka et al., 2006). H3K4 methylation is dynamically regulated by histone methylases and the recently identified demethylase lysine-specific demethylase 1 (LSD1), which mediates demethylation of H3K4me1/2, but not H3K4me3, due to the inherent chemistry (Shi et al., 2004). Given the critical role of H3K4me3 in active transcription, it is of significant interest to investigate whether there are demethylases that specifically reverse H3K4 trimethylation.

We used a candidate approach (Whetstine et al., 2006) to search for H3K4me3 histone demethylases, focusing on approximately 28 human JmjC-domain-containing

proteins. In this report, we provide both in vitro and in vivo evidence that SMCX (alias JARID1C) reverses both H3K4 tri- and dimethylation. SMCX contains the catalytic JmjC domain, JmjN, and a C5HC2 zinc finger, as well as two plant homeodomain (PHD) domains, a motif that binds methyl-lysine residues (Shi et al., 2006; Wysocka et al., 2006). Importantly, *SMCX* has recently been shown to be a causal gene for X-linked mental retardation (XLMR) (Jensen et al., 2005). XLMR is a heterogenous disease involving environmental, stochastic, and/or genetic factors. It affects 2 out of 1000 males, and the symptom ranges from mild to severe mental retardation (Ropers and Hamel, 2005). Although systematic mutation screenings have identified many genes implicated in XLMR, *SMCX* appears to be one of the more frequently mutated genes in this disease (Tzschach et al., 2006). Thirteen *SMCX* point mutations have been identified (Jensen et al., 2005; Santos et al., 2006; Tzschach et al., 2006). Most of these mutations are missense mutations, which are located near JmjN, JmjC, the C5HC2 finger, and the N-terminal PHD domain, but the molecular consequences of these mutations were unclear.

SMCX is evolutionarily conserved, and in mammals, it is a member of a subfamily of four proteins, including SMCY (JARID1D), RBP2 (JARID1A), and PLU-1 (JARID1B) (Klose et al., 2006a). The other family members are also associated with important biology and human diseases. For instance, SMCY was identified as a male-specific antigen (Agulnik et al., 1994; Scott et al., 1995; Wang et al., 1995), while RBP2 was isolated as a pRB binding protein (Defeo-Jones et al., 1991), and its inactivation was proposed to be important for pRB to promote differentiation (Benevolenskaya et al., 2005). Analysis of the fission yeast *S. pombe* homolog of RBP2, Msc1, suggested a possible role for this protein in modulating cellular response to DNA damage (Ahmed et al., 2004). Plu-1, on the other hand, has a restricted expression pattern in the testis, ovary, and transiently in the mammary gland of the pregnant female (Barrett et al., 2002) and has been shown to be upregulated in breast and testis cancer, suggesting a potential role in tumorigenesis (Lu et al., 1999). PLU-1 has also been shown to interact with the DNA binding transcription factors BF-1 and PAX9 and possibly function as a transcriptional corepressor (Tan et al., 2003). These findings suggest a link between this family of proteins with multiple biological processes and human diseases.

We show that SMCX is a H3K4 trimethyl-histone demethylase, catalyzing demethylation of H3K4me3 to H3K4me1, but having no effect on methylation at other lysine residues, including H3K9, -27, -36, and H4K20. Consistent with these observations, overexpression of SMCX resulted in a specific reduction of H3K4me3 in cultured cells. As expected, we found that the other human SMCX family members were also H3K4 demethylases. We show that one of the two PHD fingers of SMCX specifically bound H3K9me3, suggesting crosstalks between H3K4 and H3K9 methylation in transcriptional repression. Importantly, *SMCX* mutations associated with XLMR compromised the demethylase activity, as well as its ability to bind H3K9me3. These findings suggest that a reduction of SMCX demethylation function is detrimental and may be a common cause of XLMR associated with *SMCX* mutations. To gain insights into the biological context in which SMCX functions that may be relevant to understanding of its role in XLMR, we investigated SMCX in both zebrafish and mammalian neurons. In situ hybridization revealed a developmental expression profile of SMCX that is restricted to the zebrafish brain. Consistently, inhibition of smcx resulted in significant defects in neuronal development in zebrafish, including increased neuronal cell death. In addition, inhibition of *Smcx* in primary mammalian neurons impaired dendritic morphogenesis. Importantly, while an RNAi-resistant wild-type *SMCX* transgene restored dendritic growth in the background of smcx knockdown, transgenes carrying point mutations, including an XLMR-patient point mutation, that disrupt demethylase activity failed to effectively restore dendritic growth, thus linking the demethylase activity to SMCX regulation of dendritic development. Our findings thus define a family of enzymes that reverse H3K4 trimethylation and provide novel insights into the molecular mechanisms that underlie XLMR pathology.

RESULTS

SMCX Mediates Demethylation of Histone H3K4me3 and H3K4me2

SMCX (JARID1C) belongs to a small family of evolutionarily conserved proteins, whose members include RBP2 (JARID1A), PLU-1 (JARID1B), and SMCY (JARID1D) (Figure S1). The SMCX family members contain the JmjC domain, which has been shown to be the catalytic moiety for multiple histone demethylases (Chen et al., 2006; Cloos et al., 2006; Klose et al., 2006b; Tsukada et al., 2006; Whetstine et al., 2006; Yamane et al., 2006). Members of the SMCX family also contain the JmjN domain, which is conserved among a subset of JmjC-domain proteins and has recently been shown to be important for maintaining the structural integrity of the adjacent JmjC domain, and therefore is critical for catalysis (Chen et al., 2006). SMCX family members also contain a C5HC2 zinc finger located C-terminal to the JmjC domain. Although its function is unclear, a C2HC4 zinc finger has been shown to be important for JHDM2A demethylase activity (Yamane et al., 2006). All four members contain the BRIGHT domain, which is an AT-rich domain interacting domain (ARID). ARID domains have the capability of binding DNA in a sequence-specific and nonsequence specific manner (Kortschak et al., 2000; Wilsker et al., 2002), suggesting that SMCX and its related proteins may have similar properties. Finally, all four members contain the PHD domain, which has recently been shown to be a histone-methyl-lysine binding motif (Shi et al., 2006; Wysocka et al., 2006). Phylogenic analysis shows that SMCX, SMCY, and RBP2 are more similar to one another than PLU-1 (Figure S1). Importantly, the amino acids within

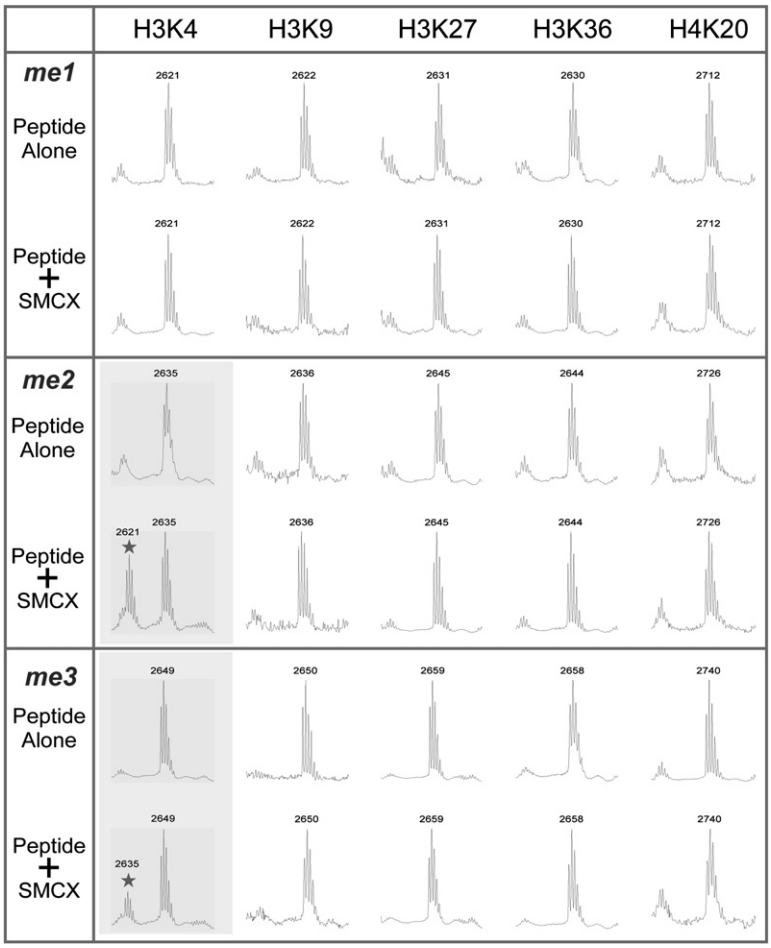

Figure 1. Histone Demethylation Mediated by the Full-Length SMCX

Mono-, di-, and trimethylated synthetic histone peptide (2 μg) were incubated with SMCX (2 μg) purified from Sf9 cells. Demethylated peptides were detected as mass peaks with the molecular weight that are 14 Da smaller than the input peptides. Demethylated peptides are marked with starred and shaded panels. Among the methylated residues examined (H3K4, -9, -27, and -36, and H4K20), SMCX removed methyl moieties only from H3K4me2 and H3K4me3.

the JmjC domain that have been shown to be critical for cofactor binding and catalysis are conserved among all four SMCX family members (data not shown).

To determine whether SMCX is a histone demethylase, we isolated a full-length SMCX cDNA from HeLa cells by RT-PCR, subcloned it into a Gateway entry vector, subsequently transferred it to a baculoviral expression vector, and purified recombinant protein to near homogeneity from insect Sf9 cells. We used a MALDI-TOF mass spectrometric approach to screen for demethylation using a variety of histone peptides representing mono-, di-, and trimethylation for four lysines on H3 and one lysine residue on H4. As shown in Figure 1, SMCX mediated demethylation at H3K4, but not H3K9, K27, K36, or H4K20. SMCX appeared to specifically demethylate H3K4me3 and H3K4me2 but not H3K4me1 (Figure 1, shaded panels), suggesting that SMCX converts H3K4 from tri- to monomethylated state. Consistent with these observations, when bulk histones were used as substrates, western blot analysis also showed SMCX-mediated demethylation of both H3K4me3 and H3K4me2 but not mono-, di-, or trimethylated H3K9 and H3K27 (Figure 2A). JmjC-domain-mediated demethylation reactions require Fe(II) and α-ketoglutarate as cofactors (Chen et al., 2006; Tsukada et al., 2006; Whetstine et al., 2006). As shown in Figure S2, omission of α-ketoglutarate, or addition of EDTA resulted in a significant inhibition of the demethylation reaction mediated by SMCX. Taken together, these findings show that SMCX mediates H3K4me3/2 demethylation using the same chemistry described for other JmjC-domain-containing histone demethylases.

Demethylation by Other Members of the SMCX Family

The finding that human SMCX is a histone demethylase prompted us to investigate whether the other three closely related family members, SMCY, RBP2, and PLU-1, were histone lysine demethylases as well. Full-length cDNAs for human SMCY and RBP2 and mouse Plu-1 were cloned into the baculoviral vector for expression in the Sf9 insect cells. Bulk histone proteins were incubated with purified RBP2, SMCY, and Plu-1, respectively. As shown in Figure 2B, while SMCY demethylated H3K4me3 and H3K4me2, PLU-1 mediated demethylation of all three methylation states of H3K4. RBP2 had barely detectable demethylase activity under the same assay condition (Figure 2B). Similar results were obtained using mass spectrometry where clear albeit low demethylase activity

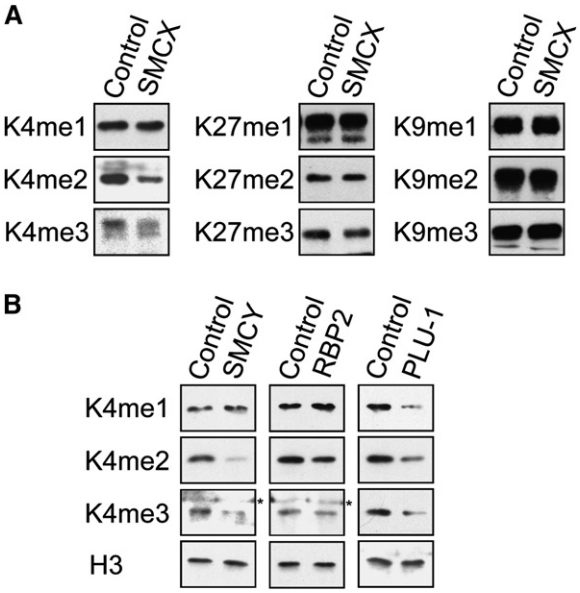

Figure 2. Specific Demethylation of Methylated H3K4 on Native Histone by SMCX, SMCY, Plu-1, and RBP2

(A and B) Calf thymus histones (3 μg) were incubated with 3 μg of purified, full-length SMCX, SMCY, RBP2, and PLU-1, respectively, and subjected to western blot analysis using antibodies that specifically recognize methylated histones. Heat-inactivated recombinant proteins were used as controls. Reduced signals were found only for H3K4me3 and H3K4me2 by SMCX and SMCY and for all three methylation states by Plu-1. Nonspecific signals were marked as asterisks.

was detected for SMCY and Plu-1, but RBP2 showed the lowest detectable activity (Figure S3). It is unclear whether low levels of activity were due to improper folding of the recombinant proteins or additional factors are needed for optimal demethylase activity. In summary, we have demonstrated that SMCX family members are histone demethylases that are mainly involved in demethylation of tri- and dimethylated H3K4.

SMCX Overexpression Antagonizes H3K4 Di- and Trimethylation In Vivo

We next investigated whether SMCX overexpression would alter H3K4 tri- and dimethylation in vivo. SMCX was fused to the HA epitope (HA-SMCX) and transfected into U2OS cells. Forty-eight hours posttransfection, cells were fixed and costained with antibodies recognizing the HA epitope and histone methylation at various lysine residues. As shown in Figure 3, the signals representing H3K4me3 and H3K4me2, but not H3K4me1, were significantly reduced in ~70% of the transfected cells where SMCX was overexpressed (panels A–I; marked by arrows). Importantly, the point mutation H514A that abrogated the demethylase activity of SMCX eliminated the ability of HA-SMCX to reduce H3K4me2/3 in vivo (less than 5% of the transfected cells exhibited reduced signals) (Figure 3; panels J–R), suggesting that the reduction of the H3K4me2/3 signals was likely due to demethylation. Taken together, these findings provide in vivo evidence that SMCX antagonizes tri- and dimethylation at H3K4, likely via enzymatic demethylation.

Analysis of Mutant SMCX Proteins Associated with XLMR

Thus far, 13 *SMCX* point mutations have been identified in the XLMR patients (Jensen et al., 2005; Santos et al., 2006; Tzschach et al., 2006). Many of these mutations are missense mutations that are located at various parts of the gene. As shown in Figure 4A, residue A388 is located near the N-terminal PHD finger of SMCX (PHD1) and is mutated to proline (A388P) in some XLMR patients (Jensen et al., 2005). Residue F642 is located near the

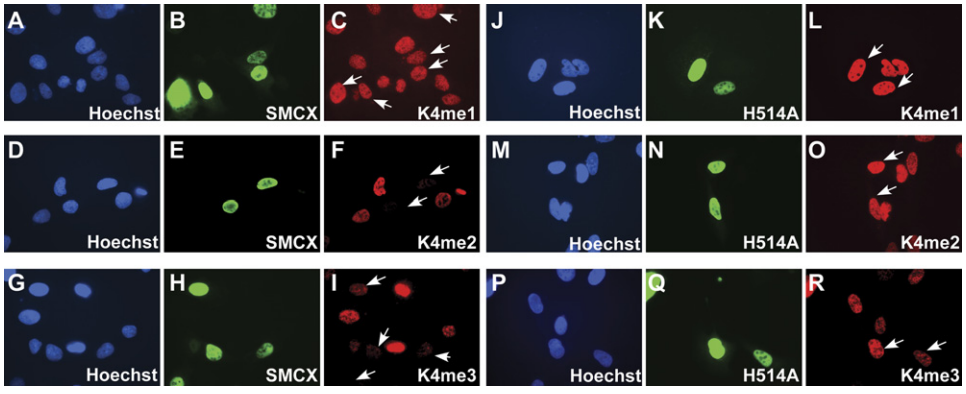

Figure 3. Overexpression of SMCX Resulted in Reduction of H3K4me2/3 Signals In Vivo

Expression construct carrying HA-SMCX (A–I) or a mutant HA-SMCX (H514A, J–R) was transiently transfected into U2OS cells and stained by anti-HA (green) and appropriate antibodies against methylated histones (H3K4me1, H3K4me2, or H3K4me3; red). Nucleus was counterstained by Hoechst 33342. Comparing to untransfected cells, significant decrease of K4me2 and K4me3 level was found in SMCX overexpressing cells (C and F, arrows). The demethylation activity was completely abrogated by H514A mutation (O and R, arrows). Overexpression of neither wild-type SMCX nor SMCX (H514A) affected the K4me1 status (C and L, arrows).

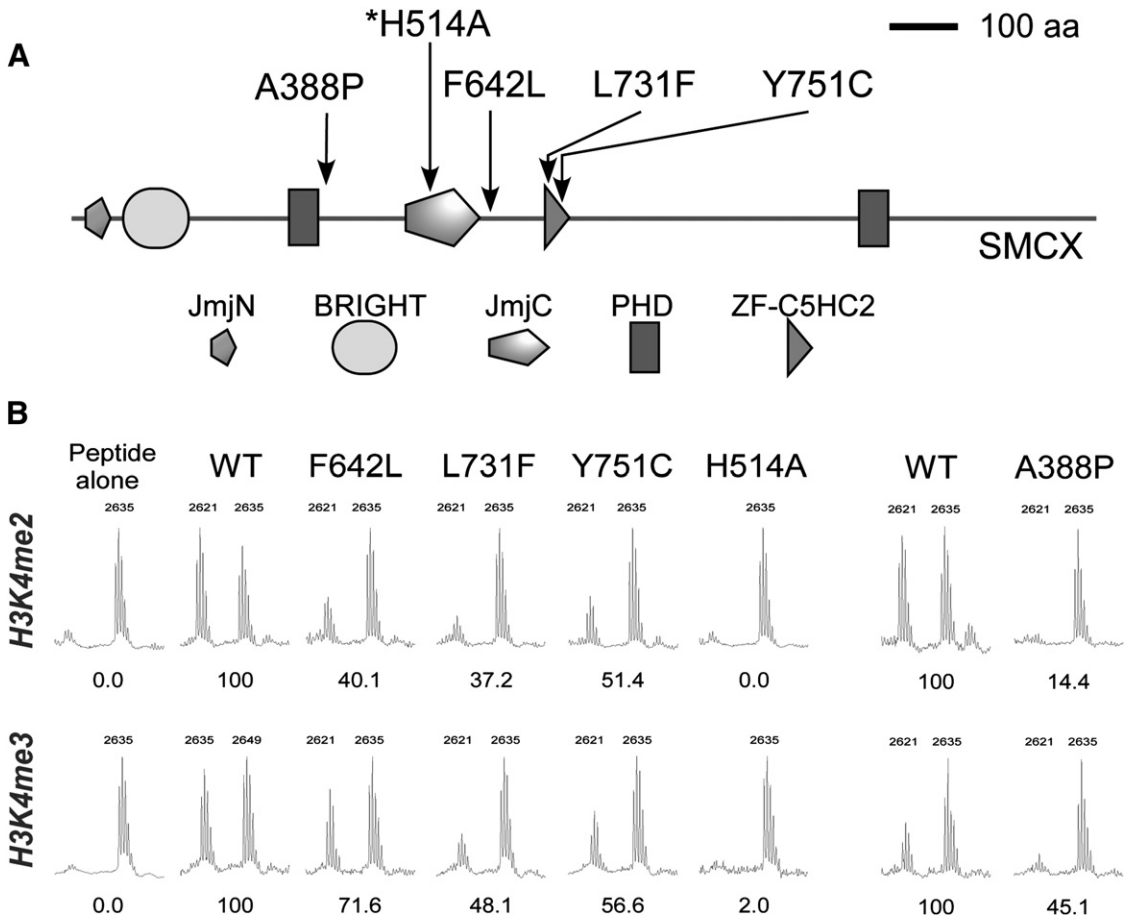

Figure 4. Histone Demethylation Activity of Mutant SMCXs Associated with X-Linked Mental Retardation (XLMR)

(A) Schematic representation of mutated amino acids of SMCX associated with XLMR that were analyzed in this study. A388P and F642L are located close to the N-terminal PHD finger and JmjC domain, respectively. L731F and Y751C are located within the C5HC2-type zinc finger motif C-terminal to the JmjC domain. H514A (denoted with an asterisk) is enzymatically inactive because histidine 514 is predicted to be critical for folding Fe(II).

(B) Histone-demethylation activity of the mutants was examined by MALDI-TOF mass spectrometry. The relative activity was calculated from the ratio of the demethylated peptide to the input uncatalyzed peptide from multiple experiments.

catalytic JmjC domain, while L731 and Y751 are located within the C5HC2 zinc finger adjacent to the JmjC domain (Figure 4A). We introduced these mutations (A338P, F642L, L731F, and Y751C) into SMCX. These mutants were expressed equally well as the wild-type protein in Sf9 cells (Figure S4). We carried out demethylation reactions with both wild-type and mutant SMCX proteins and found that these mutations reduced SMCX demethylase activity ranging from ~30%–70% of that of the wild-type enzyme (Figure 4B). Similar results were obtained using bulk histones as substrates (data not shown), suggesting that a compromised demethylase activity of SMCX may be an important and common mechanism that underlies XLMR pathology.

PHD domains have recently been shown to be a protein module that can bind methylated lysine residues (Shi et al., 2006; Wysocka et al., 2006). We asked whether the PHD domains of SMCX bound methylated lysines and whether A388P mutation might compromise binding because of its close proximity to PHD1 (Figure 4A). The two PHD domains of SMCX were subcloned into GST vector, and the fusion proteins were purified from bacteria and incubated with biotinylated histone H3 peptides that are methylated at various lysine residues. As shown in Figure 5A, PHD1 but not PHD2 of SMCX showed preferential binding to histone H3K9me3. Importantly, A388P reduced PHD1 binding to H3K9me3 by ~60%, and a representative result is shown in Figure 5B. These findings suggest that PHD1 may connect SMCX to H3K9 methylation and the patient A388P mutation potentially compromises this communication. Taken together, these findings suggest that A388P mutation affects both chromatin association and enzymatic activity.

SMCX Plays a Role in Neuronal Survival and Dendrite Development

To address the biological role of SMCX that may be relevant to our understanding of XLMR, we undertook

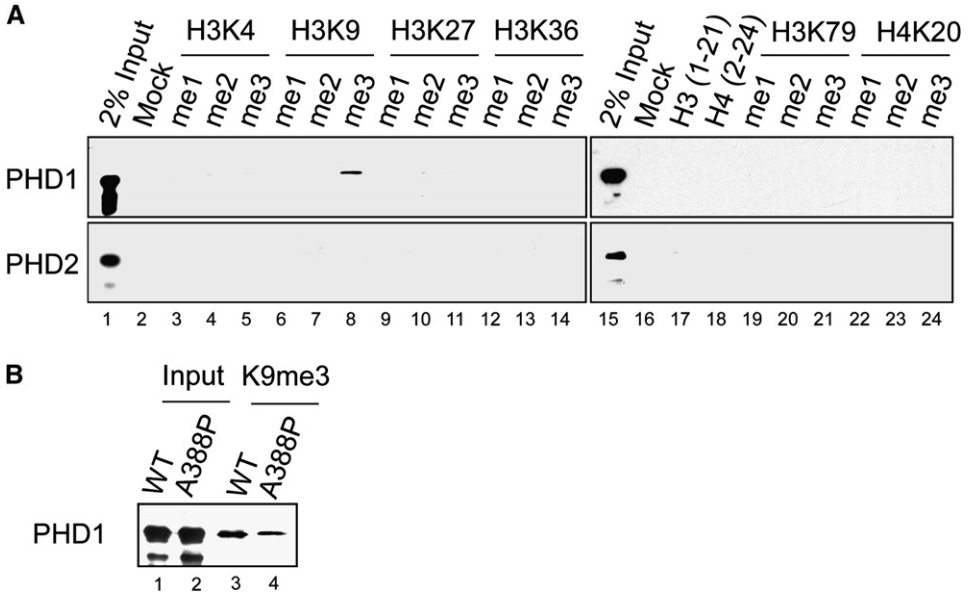

Figure 5. Recognition of H3K9me3 by a PHD Finger of SMCX

(A) Histone-peptide binding assay. Two PHD fingers of SMCX, referred as PHD1 and PHD2, were fused to GST and purified from bacteria. Biotinylated histone peptides shown in a panel were incubated with purified PHD fingers, and pulled down by streptavidin agarose. After washing, the bound GST fusion proteins were visualized by western blot analysis using anti-GST antibody. Among the differently methylated histone peptides that we tested, only H3K9me3 peptide bound PHD1. No detectable binding was found for PHD2.

(B) A388P mutation associated with X-linked mental retardation affects PHD1 binding to H3K9me3. GST-fused wild-type and mutant PHD1 carrying A388P were incubated with H3K9me3 peptide and washed four times, and the bound fractions were analyzed by western blot analysis.

analysis of *smcx* in zebrafish development. We first analyzed the developmental expression pattern of the zebrafish *smcx* homolog (XM_704687) by RNA in situ hybridization. We found *smcx* transcripts at all stages of zebrafish embryogenesis (Figure 6A). The ubiquitously expressed *smcx* transcripts detected at 2 hr postfertilization (hpf, Figure 6A; panel a) are likely to be maternal transcripts, since there is no embryonic transcription at this stage of development. During somitogenesis (12 hr, Figure 6A; panel b), *smcx* appeared to be ubiquitously expressed, with slightly stronger signal in anterior regions (future head) than in other parts of the embryo. Starting at the postsomitogenesis stage (24 hr), *smcx* was detected mainly in the brain (Figure 6A; panel c), while the neural tube and some muscle tissue were also weakly stained (Figure 6A; panel c, arrows and arrow heads, respectively). After 36 hr, *smcx* staining became entirely restricted to the head region (Figure 6A; panels d–f). Importantly, the sense probes did not yield any signals at all the corresponding stages tested (Figure 6A; panels g–l), indicating that the in situ signals (panels a–f) are specific to *smcx*. In sum, the RNA in situ results suggested that the *smcx* transcript was present throughout fish embryogenesis, with ubiquitous expression during early stages and exclusive expression in the head 36 hpf. We next analyzed Smcx function in development by using two independent morpholinos (MO) targeting *smcx*. As shown in Figure 6B, both *smcx* MOs, but not a control morpholino, resulted in neuronal developmental defects, including brain-patterning defects as well as significant neuronal cell death as shown by acridine orange positive signals. This suggests that fish Smcx plays an important role in neuronal survival, consistent with its brain-specific expression during development.

To examine whether the prosurvival role of Smcx is cell autonomous, we transplanted a small population of MO-treated cells into wild-type embryos and tracked the fate of the transplanted cells. Green and red cells, which had been treated by control MO and *smcx* MO respectively, were collected from individual 4 hpf embryos and mixed, then injected into another uninjected embryo at 5 hpf. As shown in Figure 6C, most red signal (*smcx* MO) in the head and neural tube appeared as tiny punctate spots, likely to be extracellular aggregates of dextran dye left over from degenerated cells. In contrast, green signal (control MO) stained larger neural cell bodies, many of which appear to have axons or dendrites. Furthermore, labeled cells, which had developed to other tissue lineages, such as skeletal muscle fibers, stained similarly for both green and red dyes. These data suggest that Smcx functions cell autonomously and is specifically required for neuronal cell survival and probably function.

We next characterized Smcx function in mammalian neurons. Abnormalities of neuronal morphology, and in particular of dendritic development, have been reported in brains of mental retardation, including X-linked mental retardation (Fiala et al., 2002; Ropers and Hamel, 2005). We therefore examined the role of smcx in neuronal

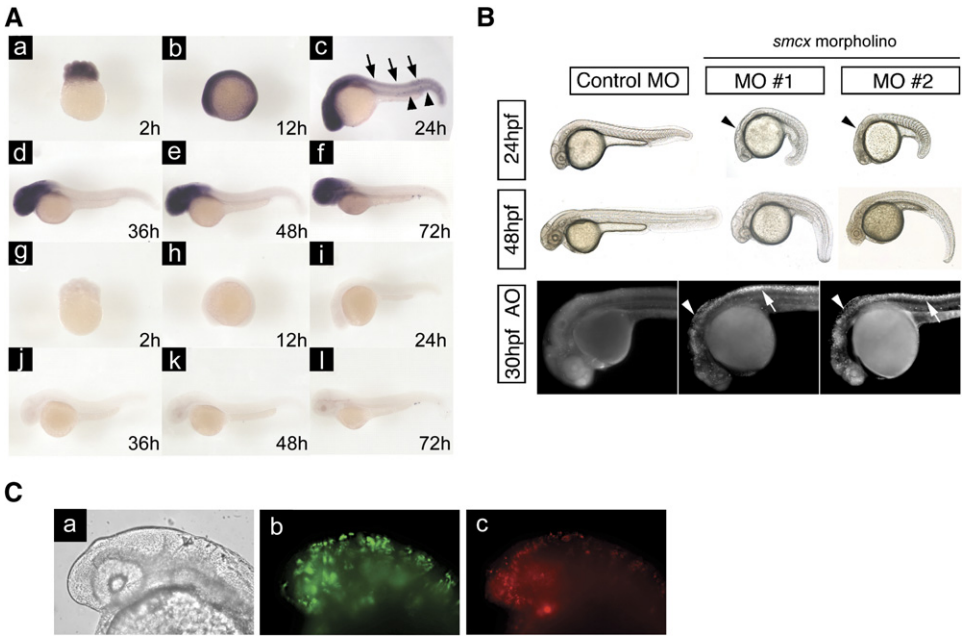

Figure 6. Brain-Specific Expression and a Role for Smcx in Neuronal Survival during Zebrafish Development

(A) RNA in situ hybridization of whole-mount zebrafish embryos. In (a–f), antisense *smcx* RNA probe hybridized with embryos at the time points indicated. Arrows point to the neural tube, and arrowheads indicate muscles that were weakly stained. In (g–l), or the control, sense *smcx* probe hybridized with embryos of the same developmental stages.

(B) Smcx is required for proper neuronal development and survival. Zebrafish embryos injected with two independent antisense morpholinos (MO 1 and 2) to *smcx* show developmental delay and have abnormal brain patterning (black arrowheads) at 24 hr postfertilization (hpf) compared with embryos injected with a control morpholino. At 48 hpf, knockdown embryos show moderate ventral curvature of the tail. Acridine orange (AO) staining at 30 hpf reveals dramatic cell death throughout the brain (white arrowheads) and neural tube (white arrows) in knockdown embryos.

(C) Transplantation of MO-treated cells to wild-type embryos. Live cell bodies labeled with green dye in the head of most morpholino-treated cells are visible, and often long neuronal processes can be observed (b). Most *smcx* MO-treated cells with red dye formed small diffuse spots, likely to be dead cell aggregates (c). Bright field view is shown in (a).

morphogenesis. Granule neurons of the rodent cerebellar cortex represent an excellent model system for the study of axonal and dendritic development (Gaudilliere et al., 2004; Konishi et al., 2004). To determine the function of endogenous Smcx in rodent neuronal morphogenesis, we used a plasmid-based method of RNAi (Sui et al., 2002) to induce the knockdown of *Smcx* in primary granule neurons cultured from postnatal day 6 rat (P6) pups. We used two plasmids encoding hairpin RNAs targeting two distinct regions of *Smcx* (U6/smcxA and U6/smcxB). Expression of these two hairpin RNAs led to efficient knockdown of *Smcx* (data not shown). We transfected P6 granule neurons with the U6/smcxA, U6/smcxB, or control U6 RNAi plasmid encoding scrambled hairpin RNAs. *Smcx* RNAi did not reduce cell survival in primary granule neurons (Figure S5A). By contrast, we found that knockdown of *Smcx* led to a significant reduction in dendritic length (Figures 7A and 7B), suggesting a requirement for Smcx in dendritic morphogenesis. To rule out the possibility that the *Smcx* knockdown-induced dendritic phenotype is a manifestation of cell death, we induced *Smcx* RNAi in primary granule neurons, in which we also expressed the antiapoptotic protein Bcl-xl (Gaudilliere et al., 2004). We found that *Smcx* knockdown significantly reduced dendritic length even in the presence of Bcl-xl (Figure S5B). Importantly, *Smcx* knockdown did not appear to reduce the length of axons (Figure S5C). Taken together, these experiments suggest that *Smcx* knockdown impairs dendritic development independently of a potential effect of SMCX on cell survival.

To rule out the possibility that *Smcx* knockdown impairs dendritic development as a result of nonspecific activation of the RNAi machinery or off-target effects of *Smcx* RNAi, we performed a rescue experiment. We expressed a wild-type human SMCX protein encoded by cDNA designed to be RNAi resistant in the background of *Smcx* RNAi (SMCX-Res, data not shown). We found that expression of SMCX-Res in primary neurons significantly increased dendritic length in the background of *Smcx* RNAi, thus reversing the *Smcx* knockdown-induced dendritic loss (Figure 7C). Importantly, SMCX-Res proteins containing point mutations that compromise the demethylase activity (H514A), including a patient-linked mutation (F642L), failed to effectively increase dendritic length in the background of *Smcx* knockdown (Figure 7C). As controls, RNA-resistant WT, H514A, and F642L SMCX were expressed at comparable levels in 293T cells as well as cerebellar granule neurons (Figure S6). Collectively, these

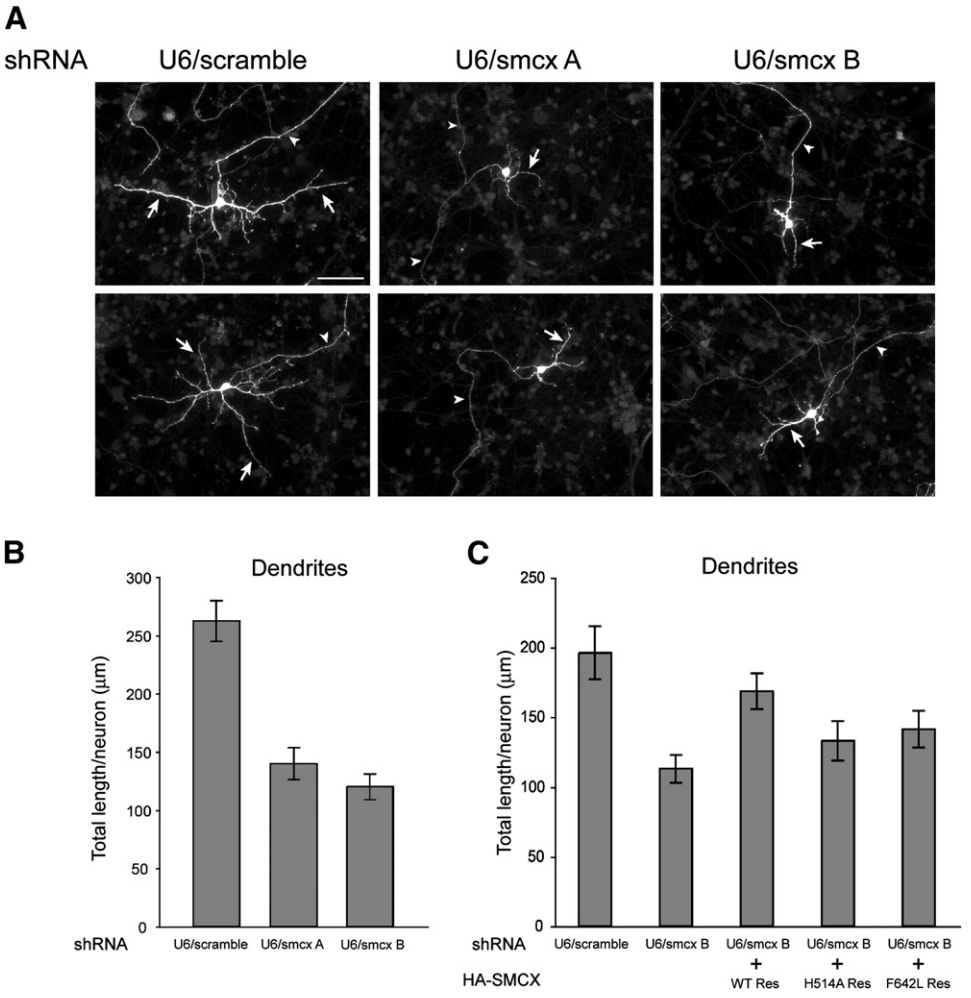

Figure 7. Smcx Is Required for Dendritic Development in Rat Cerebellar Granule Neuron

(A) Representative images of primary cultured rat cerebellar granule neurons, which were cotransfected with the U6/scramble, U6/smcxA, or U6/smcxB shRNA plasmid and a GFP expression vector and subjected to immunocytochemistry with a GFP antibody. Arrows and arrowheads indicate dendrites and axons, respectively. Scale bar denotes 50 μm.

(B) Analysis of dendritic length of neurons transfected in (A) shows that knockdown of Smcx led to a significant decrease in total dendritic length with two different RNA hairpins ($p < 0.0001$; ANOVA followed by Bonferonni-Dunn posthoc test, 160 neurons measured). Data presented as mean ± SEM.

(C) SMCX-dependent dendritic morphogenesis is linked to SMCX demethylase activity. Primary granule neurons were transfected with U6/scramble or U6/smcx B RNAi plasmid, together with a control expression vector or an expression plasmid encoding the RNAi-resistant human SMCX protein (WT Res) or point mutants that disrupt demethylase activity (H514A Res and F642L Res). Dendritic length was significantly reduced in Smcx knockdown neurons as compared to U6/scramble-transfected neurons ($p < 0.0001$; ANOVA followed by Bonferonni-Dunn posthoc test). Dendritic length was significantly increased in neurons expressing WT Res SMCX, but not in H514A Res- or F642L Res-expressing neurons, in the background of Smcx RNAi, as compared to Smcx RNAi alone ($p < 0.0041$; ANOVA followed by Bonferonni-Dunn posthoc test). Total number of neurons measured was 265. Data presented as mean ± SEM.

results indicate that *Smcx* RNAi triggers dendritic loss via specific knockdown of *Smcx* and that the demethylase activity of SMCX plays an important role in SMCX-dependent dendritic morphogenesis.

DISCUSSION

The recent discovery of LSD1, which mediates demethylation of only mono- and dimethylated histone H3K4, raised the question of whether H3K4 trimethylation is also reversible by enzymes. This was an important question since H3K4 trimethylation is intimately linked to active transcription. The finding of the SMCX/JARID1C family of demethylases that reverse H3K4 trimethylation has filled this gap and uncovered the highly dynamic nature of H3K4 methylation. Importantly, we have also provided evidence that revealed the molecular basis for the SMCX defects associated with X-linked mental retardation (XLMR) as well as a biological role for SMCX in neuronal survival and dendritic development, which may be relevant to

understanding XLMR. Collectively, our findings have provided significant new insights into XLMR by linking aberrant histone methylation to this disease.

H3K4 Methylation Regulation

At least eight histone methyltransferases have been found to mediate H3K4 methylation. Until now, LSD1 was the only H3K4 demethylase, and its enzymatic function is chemically restricted to the reversal of only mono- and dimethylated H3K4 (Shi et al., 2004). This study has identified four additional H3K4 demethylases and demonstrated that, together with LSD1, these five enzymes can reverse all three methylation states of H3K4. It also raises the possibility of a functional collaboration between LSD1 and the SMCX family of H3K4 trimethyl demethylases in the regulation of H3K4 methylation.

Previous studies of the JMJD2 subfamily of histone demethylases identified differential activities among the members toward different methylation states of H3K9. For instance, while JMJD2A mainly demethylates H3K9me3 to H3K9me2, JMJD2D is capable of demethylating H3K9me3 to H3K9me1 (Whetstine et al., 2006). This is likely to be due to the fact that these enzymes have differential capabilities of recognizing different numbers of methyl groups, a hypothesis that is supported by the identification of a methyl-group binding pocket within the catalytic center of these enzymes (Chen et al., 2006). The SMCX family of H3K4 demethylases also appears to have differential methyl-group specificities. While SMCX catalyzed H3K4me3 to H3K4me1, Plu-1 reversed H3K4me3 to unmethylated product, which further supports the hypothesis that demethylases may provide a fine-tuning mechanism for histone methylation regulation (Whetstine et al., 2006).

SMCX and XLMR

An important insight that this study has provided is the link between histone methylation and XLMR. Until this study, the molecular basis for XLMR pathology associated with SMCX mutations was unknown. The finding that SMCX mutations compromised the demethylase activity suggests that XLMR may be in part caused by aberrant histone methylation as a result of mutations of the demethylase SMCX. The finding that the N-terminal PHD finger of SMCX specifically recognizes H3K9me3 is interesting, particularly in light of the fact that the A338P mutation compromised this interaction, which suggests the functional importance of binding of SMCX to H3K9me3. We speculate that this interaction may help direct SMCX to and/or stabilize SMCX at its target genomic locales, and the PHD domain may provide a means of a functional crosstalk between SMCX and H3K9 trimethylation in the establishment of a repressive chromatin environment. A similar observation has been made for JMJD2A, which demethylates H3K9me3 and H3K36me3 (Klose et al., 2006b; Whetstine et al., 2006), but its double Tudor domain binds methylated H3K4 (Huang et al., 2006). Therefore, crosstalks among different modifications may be a common mechanism for histone-modifying enzymes to mount a coordinated regulation of chromatin structure and transcription.

Many genes have been identified to be involved in XLMR (Chelly and Mandel, 2001; Ropers, 2006; Ropers and Hamel, 2005). A subset of these genes seem to be involved in nuclear functions, which include DNA binding transcription factors such as the homeobox and zinc finger proteins ARX and ZNF41 as well as chromatin-remodeling proteins such as MeCP2 and SMCX. A number of kinases have also been implicated in XLMR, including RSK2 and STK9/CDK5L as well as regulators of the rhoGTPases (Ropers and Hamel, 2005). It is unclear whether the kinases and transcriptional regulators associated with XLMR are components of the same regulatory pathway. It is interesting to note that in addition to SMCX, PHF8, which is a JmjC-domain protein and a histone-demethylase candidate, is implicated in XLMR, suggesting possible functional interactions between these histone demethylases. Lastly, MeCP2, which is a methyl-CpG binding protein, is also an XLMR gene (Ropers and Hamel, 2005), suggesting possible interactions between histone and DNA methylation in XLMR.

The biological processes regulated by SMCX were unknown and may help shed light on mechanisms by which a defective SMCX causes XLMR. We found expression of the zebrafish *smcx* homolog during development to be largely restricted to the brain (Figure 6A). Consistent with this tissue-specific expression pattern, the zebrafish experiments identified a role for Smcx in neuronal survival (Figure 6B), suggesting that increased neuronal cell death may be associated with XLMR. The neuronal phenotypes are most likely due to *smcx* knockdown because the two independent *smcx* morpholinos with nonoverlapping transcript targets yielded the same phenotypes. These two morpholinos are designed specifically for *smcx* and bear no sequence similarity to other members of the *jarid1* family or JmjC-domain histone demethylases in general. Furthermore, several morpholinos designed for other zebrafish *smcx* family members resulted in phenotypes that are distinct from those of the *smcx* morpholinos-treated animals (not shown).

The identification of a role for Smcx in dendritic development is of particular interest (Figures 7A–7C) since abnormalities of dendritic spines, which are specialized postsynaptic regions of dendrites in distinct populations of neurons, are found in the brains of mental-retardation patients (Govek et al., 2004). The absence of a cell-survival phenotype upon *Smcx* RNAi in primary mammalian cerebellar granule neurons (Figure S5), as compared to Smcx's prosurvival function revealed in the zebrafish nervous system, could be due to the differing levels of *Smcx* knockdown. Alternatively, it could be due to distinct model systems and processes (neural development versus postmitotic neuronal morphogenesis), suggesting that SMCX may be a versatile epigenetic modifier that influences diverse biological functions in neurons. The ability of an RNAi-resistant human *SMCX* transgene to

rescue the *Smcx* knockdown-induced dendritic phenotype indicates that the observed phenotype is the result of specific *Smcx* knockdown rather than potential off-target effects of RNAi (Figure 7C). Importantly, the compromised ability of the catalytically impaired SMCX (including a patient-linked XLMR point mutation) to rescue the dendritic phenotype provides a link between the demethylase activity and the regulation of dendritic development by SMCX (Figure 7C). Overexpression of wild-type SMCX did not appear to affect dendrite length, supporting the idea that the loss of SMCX function is relevant to neuronal dysfunction (Figure S5D). In future studies, it will be important to determine SMCX function in the later phases of dendritic development in the mammalian brain including those that are intimately linked with postsynaptic dendritic morphogenesis.

In summary, we have identified a new family of histone demethylases with specificity toward tri- and dimethylated H3K4. Importantly, we have shown that XLMR-patient point mutations compromised the demethylase activity of SMCX, thus providing new insights into mechanisms that underlie XLMR. Furthermore, the finding of SMCX in neuronal survival and dendritic development with a potential link to the demethylase activity of SMCX provides a biological framework for XLMR. Lastly, since other members of the SMCX family have been implicated in differentiation and tumorigenesis, the identification of these proteins as histone demethylases suggests that misregulation of H3K4 methylation may impact multiple biological processes, resulting in human pathological conditions including XLMR and cancer.

EXPERIMENTAL PROCEDURES

Peptides and Antibodies

Biotinylated histone peptides were purchased from AnaSpec. Antibodies (Ab) that recognize different histone modifications were purchased from Upstate Group, Inc., including anti-H3K4me1 Ab (07-436), anti-H3K4me2 (07-427), anti-H3K4me3 Ab (07-473), anti-H3K9me1 (07-450), anti-H3K9me2 (07-441), anti-H3K9me3 (07-442), anti-H3K27me1 (07-448), anti-H3K27me2 (07-452), anti-H3-K27me3 (07-449), and anti-panH3 (06-775).

Expression Plasmids

SMCX, *SMCY*, and *RBP2* were PCR amplified from cDNA libraries (HeLa, brain, lung, and testis) using Phusion polymerase (Finnenzymes) and cloned into the Gateway Entry System (Invitrogen). Full-length cDNA of mouse Plu-1 (MGC: 61207) was purchased from Invitrogen. A fully sequenced cDNA, as well as the *SMCX* mutants, A388P, F642L, L731F, Y751C, and H514A generated by PCR, were transferred into additional Gateway HA-tag and FLAG-baculoviral expression vectors. The SMCX-PHD1 and PHD2 were cloned into pGEX4T-1 (Amersham) for expression as GST fusion proteins in bacteria.

Purification of FLAG-SMCX and Demethylation Reactions

The FLAG-tagged proteins were expressed in Sf9 cells using BAC-N-BLUE baculoviral expression system (Invitrogen). Cells were lysed in 20 mM Tris-HCl (pH 7.5), 150 mM NaCl, 0.1% NP-40, 0.2% Triton X-100, 1 mM DTT, 1 mM PMSF, and Protease Inhibitor Cocktail (Roche). Recombinant proteins were immobilized on FLAG M2 affinity gel (Sigma), washed with buffer W (20 mM Tris-HCl [pH 7.5], 150 mM NaCl, 8.0% glycerol, 1 mM DTT, 0.01% NP40), and eluted in buffer W containing 100 μg/ml of 3x FLAG peptide (Sigma). Purified proteins were incubated with 2 μg of histone peptides or 3 μg of calf type II-A histone (Sigma) in the DeMTase reaction buffer (20 mM Tris-HCl [pH7.5], 150 mM NaCl, 50 μM $[NH_4]_2Fe[SO_4]_2$, 1 mM α-ketoglutarate, and 2 mM ascorbic acid) for 2–5 hr at 37°C. A total of 2–7.5 μg of full-length SMCX were added to the reactions. The reactions were inhibited by 500 μM EDTA.

MALDI-TOF Mass Spectrometry

One microliter of the 50 μl demethylation reaction mixture was desalted through a C18 ZipTip (Millipore). The ZipTip was activated, equilibrated, and loaded as previously described by Shi et al. (2004). The bound material was then eluted with 10 mg/ml α-cyano-4-hydroxycinnamic acid MALDI matrix in 70% acetonitrile/0.1% TFA before being spotted and cocrystallized. The samples were analyzed by a MALDI-TOF mass spectrometer.

Immunofluorescence Microscopy

U2OS cells were plated on coverslips in 24-well dishes (5.0×10^5 cells/well), and expression plasmids carrying HA-SMCX or HA-SMCX H514A were transfected with Lipofectamine 2000 (Invitrogen) according to the manufacturer's instructions. Forty-eight hours later, cells were fixed with 4% paraformaldehyde, permeabilized, and blocked with 10% fetal bovine serum (FBS). The coverslips were incubated for 3 hr at room temperature with the appropriate primary antibodies, washed, and incubated with the corresponding secondary antibodies for 1 hr at room temperature. The coverslips were then washed, mounted with Vectashield (Vector Laboratories), and analyzed by a fluorescence microscopy (Nikon E600) using a 60x objective. Images were acquired and processed with Openlab 3.1.5 software. Primary antibodies were used at the following dilutions: 1:1,000 anti-HA (Covance monoclonal HA.11), 1:1,000 anti-H3K4me1 (Upstate 07-436), 1:3,000 anti-H3K4me2 (Upstate 07-030), and 1:25,000 anti-H3K4me3 (Upstate 07-473). Alexa 594-conjgated donkey-anti-rabbit and Alexa 488-conjugated goat-anti-mouse secondary antibodies (Molecular probes) were used at 1:500. Hoechst 33342 was used with all nuclear staining.

Histone Peptide Binding Assay

GST-fused PHD1 and PHD2, which correspond to 261–414 and 1146–1267 amino acids, respectively, were expressed in *E. coli* strain JM109 and purified by glutathione-affinity resin (Amersham). Five micrograms of purified proteins were incubated with 0.2 μg of biotinylated histone peptide in 100 μl of the binding buffer (50 mM Tris-HCl [pH7.5], 150 mM NaCl, 0.05% NP-40, 0.3 mg/ml BSA) overnight at 4°C. Protein-peptide complexes were pulled down with streptavidin beads (Upstate), washed five times, and subjected to western blot analysis using anti-GST antibody (B-14, Santa Cruz, CA).

In Situ Hybridization

Whole-mount zebrafish embryo in situ hybridizations using *smcx* digoxigenin-labeled antisense and sense RNA probes were carried out following the method described previously (Chan et al., 2001).

Knockdown of Zebrafish *smcx* Homolog and Phenotypic Analysis

Knockdown of zebrafish *smcx* was performed by injection of 2 nl of a stock concentration of 250 μM antisense morpholinos (Gene-Tools, LLC) into one-cell stage zebrafish embryos using a gas-driven microinjector (Medical Systems Corp.). The morpholino sequences used were 5′-CAAACTCCTCCCCTACATCCATCAT-3′ covering transcript bases −3 to +22 of translated sequence, and 5′-TGAGTTCTTCTT ATTCTTCGGTGAC-3′, covering −46 to −22 of translated sequence or a control morpholino of the sequence 5′-CCTCTTACCTCAGTTA CAATTTATA-3′. For in vivo detection of cell death, live 30-hr-old embryos were incubated in 2 μg/ml acridine orange (Sigma) in embryo

media in the dark for 30 min and washed three times in fresh embryo media, and fluorescence was observed under 488 nm wavelength excitation. Cell-transplantation experiments were performed essentially as described (Yin and Solnica-Krezel, 2006). Briefly, control MO and *smcx* MO were coinjected with green and red fluorescent 10 kDa dextrans, respectively, into one-cell stage wild-type embryos, and the embryos were cultured to the blastula stage where cells are still pluripotent (4 hpf). We collected the green (control) and red (*smcx* MO) cells from individual embryos and mixed them; then, we injected ~20–40 cells of the mixture into another previously uninjected wild-type embryo at a slightly later stage (5 hpf). The MO-treated cell fates were tracked using an epifluorescence microscope at 30 hpf.

Primary Granule Neuron Transfection and Immunocytochemistry

Primary cerebellar granule neurons were prepared from P6 Long Evans rat pups as described (Konishi et al., 2002). Transfections were performed using a modified calcium phosphate method 8 hr after plating (Konishi et al., 2002). Neurons were kept in medium supplemented with 10% calf serum and KCl (25 mM). To prevent glial proliferation, neurons were treated with 10 μM cytosine arabinofuranoside (AraC). A GFP expression plasmid was cotransfected in all experiments to reveal neuronal morphology. Cells were fixed 4 days after plating and subjected to immunocytochemistry with antibodies directed to GFP (Molecular Probes) and stained with the DNA binding dye bisbenzimide (Hoechst 33258).

Morphological Analysis of Cerebellar Granule Neurons

To study dendritic and axonal morphology of granule neurons in primary cultures, individual images were captured randomly on a Nikon eclipse TE2000U epifluorescence microscope using a digital CCD camera (Diagnostic Instruments). Images were imported into the Spot Imaging Software (Diagnostic Instruments), and length of neurites was analyzed by tracing. Total dendrite length refers to the length of all dendrites and branches of a given neuron added together. The same definition was used for axonal morphometry.

Supplemental Data

Supplemental Data include six figures and can be found with this article online at http://www.cell.com/cgi/content/full/128/6/1077/DC1/.

ACKNOWLEDGMENTS

We thank Gongyi Zhang, Lars Riff Jensen, and Andreas Kuß for helpful discussion. J.R.W. and L.T.U. are recipients of the Ruth L. Kirschstein National Service Award (GM 70095) and National Science Foundation Fellowship, respectively. This work was supported by grants from the National Institutes of Health (NS051255 and NS41021 to A.B.; and GM 58012, GM 071004, and NCI118487 to Y.S.), a postdoctoral fellowship from Canadian Institute of Health Research (CIHR to H.H.Q.), and in part by a grant from the Novartis Biomedical Research Institute to Y.S.

Received: October 27, 2006
Revised: January 16, 2007
Accepted: February 9, 2007
Published online: February 22, 2007

REFERENCES

Agulnik, A.I., Mitchell, M.J., Lerner, J.L., Woods, D.R., and Bishop, C.E. (1994). A mouse Y chromosome gene encoded by a region essential for spermatogenesis and expression of male-specific minor histocompatibility antigens. Hum. Mol. Genet. *3*, 873–878.

Ahmed, S., Palermo, C., Wan, S., and Walworth, N.C. (2004). A novel protein with similarities to Rb binding protein 2 compensates for loss of Chk1 function and affects histone modification in fission yeast. Mol. Cell. Biol. *24*, 3660–3669.

Barrett, A., Madsen, B., Copier, J., Lu, P.J., Cooper, L., Scibetta, A.G., Burchell, J., and Taylor-Papadimitriou, J. (2002). PLU-1 nuclear protein, which is upregulated in breast cancer, shows restricted expression in normal human adult tissues: a new cancer/testis antigen? Int. J. Cancer *101*, 581–588.

Benevolenskaya, E.V., Murray, H.L., Branton, P., Young, R.A., and Kaelin, W.G., Jr. (2005). Binding of pRB to the PHD protein RBP2 promotes cellular differentiation. Mol. Cell *18*, 623–635.

Chelly, J., and Mandel, J.L. (2001). Monogenic causes of X-linked mental retardation. Nat. Rev. Genet. *2*, 669–680.

Chan, J., Mably, J.D., Serluca, F.C., Chen, J.N., Goldstein, N.B., Thomas, M.C., Cleary, J.A., Brennan, C., Fishman, M.C., and Roberts, T.M. (2001). Morphogenesis of prechordal plate and notochord requires intact Eph/eprin B signaling. Dev. Biol. *234*, 470–482.

Chen, Z., Zang, J., Whetstine, J., Hong, X., Davrazou, F., Kutateladze, T.G., Simpson, M., Mao, Q., Pan, C.H., Dai, S., et al. (2006). Structural insights into histone demethylation by JMJD2 family members. Cell *125*, 691–702.

Cloos, P.A., Christensen, J., Agger, K., Maiolica, A., Rappsilber, J., Antal, T., Hansen, K.H., and Helin, K. (2006). The putative oncogene GASC1 demethylates tri- and dimethylated lysine 9 on histone H3. Nature *442*, 307–311.

Defeo-Jones, D., Haung, P.S., Jones, R.E., Haskell, K.M., Vuocolo, G.A., Hanobik, M.G., Huber, H.E., and Oliff, A. (1991). Cloning of cDNAs for cellular proteins that binds to the retinoblastoma gene product. Nature *352*, 251–254.

Fiala, J.C., Spacek, J., and Harris, K.M. (2002). Dendritic spine pathology: cause or consequence of neurological disorders? Brain Res. Brain Res. Rev. *39*, 29–54.

Fodor, B.D., Kubicek, S., Yonezawa, M., O'Sullivan, R.J., Sengupta, R., Perez-Burgos, L., Opravil, S., Mechtler, K., Schotta, G., and Jenuwein, T. (2006). Jmjd2b antagonizes H3K9 trimethylation at pericentric heterochromatin in mammalian cells. Genes Dev. *20*, 1557–1562.

Gaudilliere, B., Konishi, Y., de la Iglesia, N., Yao, G., and Bonni, A. (2004). A CaMKII-NeuroD signaling pathway specifies dendritic morphogenesis. Neuron *41*, 229–241.

Govek, E.E., Newey, S.E., Akerman, C.J., Cross, J.R., Van der Veken, L., and Van Aelst, L. (2004). The X-linked mental retardation protein oligophrenin-1 is required for dendritic spine morphogenesis. Nat. Neurosci. *7*, 364–372.

Huang, Y., Fang, J., Bedford, M.T., Zhang, Y., and Xu, R.M. (2006). Recognition of histone H3 lysine-4 methylation by the double tudor domain of JMJD2A. Science *312*, 748–751.

Jensen, L.R., Amende, M., Gurok, U., Moser, B., Gimmel, V., Tzschach, A., Janecke, A.R., Tariverdian, G., Chelly, J., Fryns, J.P., et al. (2005). Mutations in the JARID1C gene, which is involved in transcriptional regulation and chromatin remodeling, cause X-linked mental retardation. Am. J. Hum. Genet. *76*, 227–236.

Jenuwein, T., and Allis, C.D. (2001). Translating the histone code. Science *293*, 1074–1080.

Klose, R.J., Kallin, E.M., and Zhang, Y. (2006a). JmjC-domain-containing proteins and histone demethylation. Nat. Rev. Genet. *7*, 715–727.

Klose, R.J., Yamane, K., Bae, Y., Zhang, D., Erdjument-Bromage, H., Tempst, P., Wong, J., and Zhang, Y. (2006b). The transcriptional repressor JHDM3A demethylates trimethyl histone H3 lysine 9 and lysine 36. Nature *442*, 312–316.

Konishi, Y., Lehtinen, M., Donovan, N., and Bonni, A. (2002). Cdc2 phosphorylation of BAD links the cell cycle to the cell death machinery. Mol. Cell *9*, 1005–1016.

Konishi, Y., Stegmuller, J., Matsuda, T., Bonni, S., and Bonni, A. (2004). Cdh1-APC controls axonal growth and patterning in the mammalian brain. Science *303*, 1026–1030.

Kortschak, R.D., Tucker, P.W., and Saint, R. (2000). ARID proteins come in from the desert. Trends Biochem. Sci. *25*, 294–299.

Liang, G., Lin, J.C., Wei, V., Yoo, C., Cheng, J.C., Nguyen, C.T., Weisenberger, D.J., Egger, G., Takai, D., Gonzales, F.A., and Jones, P.A. (2004). Distinct localization of histone H3 acetylation and H3-K4 methylation to the transcription start sites in the human genome. Proc. Natl. Acad. Sci. USA *101*, 7357–7362.

Litt, M.D., Simpson, M., Gaszner, M., Allis, C.D., and Felsenfeld, G. (2001). Correlation between histone lysine methylation and developmental changes at the chicken beta-globin locus. Science *293*, 2453–2455.

Lu, P.J., Sundquist, K., Baeckstrom, D., Poulsom, R., Hanby, A., Meier-Ewert, S., Jones, T., Mitchell, M., Pitha-Rowe, P., Freemont, P., and Taylor-Papadimitriou, J. (1999). A novel gene (PLU-1) containing highly conserved putative DNA/chromatin binding motifs is specifically up-regulated in breast cancer. J. Biol. Chem. *274*, 15633–15645.

Margueron, R., Trojer, P., and Reinberg, D. (2005). The key to development: interpreting the histone code? Curr. Opin. Genet. Dev. *15*, 163–176.

Martin, C., and Zhang, Y. (2005). The diverse functions of histone lysine methylation. Nat. Rev. Mol. Cell Biol. *6*, 838–849.

Metzger, E., Wissmann, M., Yin, N., Muller, J.M., Schneider, R., Peters, A.H., Gunther, T., Buettner, R., and Schule, R. (2005). LSD1 demethylates repressive histone marks to promote androgen-receptor-dependent transcription. Nature *437*, 436–439.

Noma, K., Allis, C.D., and Grewal, S.I. (2001). Transitions in distinct histone H3 methylation patterns at the heterochromatin domain boundaries. Science *293*, 1150–1155.

Ropers, H.H. (2006). X-linked mental retardation: many genes for a complex disorder. Curr. Opin. Genet. Dev. *16*, 260–269.

Ropers, H.H., and Hamel, B.C. (2005). X-linked mental retardation. Nat. Rev. Genet. *6*, 46–57.

Sanders, S.L., Portoso, M., Mata, J., Bahler, J., Allshire, R.C., and Kouzarides, T. (2004). Methylation of histone H4 lysine 20 controls recruitment of Crb2 to sites of DNA damage. Cell *119*, 603–614.

Santos, C., Rodriguez-Revenga, L., Madrigal, I., Badenas, C., Pineda, M., and Mila, M. (2006). A novel mutation in JARID1C gene associated with mental retardation. Eur. J. Hum. Genet. *14*, 583–586.

Santos-Rosa, H., Schneider, R., Bannister, A.J., Sherriff, J., Bernstein, B.E., Emre, N.C., Schreiber, S.L., Mellor, J., and Kouzarides, T. (2002). Active genes are tri-methylated at K4 of histone H3. Nature *419*, 407–411.

Santos-Rosa, H., Schneider, R., Bernstein, B.E., Karabetsou, N., Morillon, A., Weise, C., Schreiber, S.L., Mellor, J., and Kouzarides, T. (2003). Methylation of histone H3 K4 mediates association of the Isw1p ATPase with chromatin. Mol. Cell *12*, 1325–1332.

Schneider, R., Bannister, A.J., Myers, F.A., Thorne, A.W., Crane-Robinson, C., and Kouzarides, T. (2004). Histone H3 lysine 4 methylation patterns in higher eukaryotic genes. Nat. Cell Biol. *6*, 73–77.

Scott, D.M., Ehrmann, I.E., Ellis, P.S., Bishop, C.E., Agulnik, A.I., Simpson, E., and Mitchell, M.J. (1995). Identification of a mouse male-specific transplantation antigen, H-Y. Nature *376*, 695–698.

Shi, X., Hong, T., Walter, K.L., Ewalt, M., Michishita, E., Hung, T., Carney, D., Pena, P., Lan, F., Kaadige, M.R., et al. (2006). ING2 PHD domain links histone H3 lysine 4 methylation to active gene repression. Nature *442*, 96–99.

Shi, Y., Lan, F., Matson, C., Mulligan, P., Whetstine, J.R., Cole, P.A., Casero, R.A., and Shi, Y. (2004). Histone demethylation mediated by the nuclear amine oxidase homolog LSD1. Cell *119*, 941–953.

Strahl, B.D., and Allis, C.D. (2000). The language of covalent histone modifications. Nature *403*, 41–45.

Sui, G.C., Soohoo, C., Affar, E.B., Gay, F., Forrester, W., and Shi, Y. (2002). A DNA vector-based RNAi technology to suppress gene expression in mammalian cells. Proc. Natl. Acad. Sci. USA *99*, 5515–5520.

Tan, K., Shaw, A.L., Madsen, B., Jensen, K., Taylor-Papadimitriou, J., and Freemont, P.S. (2003). Human PLU-1 has transcriptional repression properties and interacts with the developmental transcription factors BF-1 and PAX9. J. Biol. Chem. *278*, 20507–20513.

Tsukada, Y., Fang, J., Erdjument-Bromage, H., Warren, M.E., Borchers, C.H., Tempst, P., and Zhang, Y. (2006). Histone demethylation by a family of JmjC domain-containing proteins. Nature *439*, 811–816.

Tzschach, A., Lenzner, S., Moser, B., Reinhardt, R., Chelly, J., Fryns, J.P., Kleefstra, T., Raynaud, M., Turner, G., Ropers, H.H., et al. (2006). Novel JARID1C/SMCX mutations in patients with X-linked mental retardation. Hum. Mutat. *27*, 389.

Wang, W., Meadows, L.R., den Haan, J.M., Sherman, N.E., Chen, Y., Blokland, E., Shabanowitz, J., Agulnik, A.I., Hendrickson, R.C., Bishop, C.E., et al. (1995). Human H-Y: a male-specific histocompatibility antigen derived from the SMCY protein. Science *269*, 1588–1590.

Whetstine, J.R., Nottke, A., Lan, F., Huarte, M., Smolikov, S., Chen, Z., Spooner, E., Li, E., Zhang, G., Colaiacovo, M., and Shi, Y. (2006). Reversal of histone lysine trimethylation by the JMJD2 family of histone demethylases. Cell *125*, 467–481.

Wilsker, D., Patsialou, A., Dallas, P.B., and Moran, E. (2002). ARID proteins: a diverse family of DNA binding proteins implicated in the control of cell growth, differentiation, and development. Cell Growth Differ. *13*, 95–106.

Wysocka, J., Swigut, T., Xiao, H., Milne, T.A., Kwon, S.Y., Landry, J., Kauer, M., Tackett, A.J., Chait, B.T., Badenhorst, P., et al. (2006). A PHD finger of NURF couples histone H3 lysine 4 trimethylation with chromatin remodelling. Nature *442*, 86–90.

Yamane, K., Toumazou, C., Tsukada, Y., Erdjument-Bromage, H., Tempst, P., Wong, J., and Zhang, Y. (2006). JHDM2A, a JmjC-containing H3K9 demethylase, facilitates transcription activation by androgen receptor. Cell *125*, 483–495.

Yin, C.Y., and Solnica-Krezel, L. (2006). Convergence and extension movements mediate the specification and fate maintenance of zebrafish slow muscle precursors. Dev. Biol., in press. Published online December 19, 2006.

Zhang, Y., and Reinberg, D. (2001). Transcriptin regulation by histone methylation: interplay between different covalent modifications of the core histone tails. Genes Dev. *15*, 2343–2360.